

Article

Transcriptomics Analysis of Tomato Ripening Regulated by Carbon Dioxide

Jamshed Bobokalonov ^{1,2} , Yanhong Liu ³ , Karley K. Mahalak ¹, Jenni A. Firman ¹, Shiohshuh Sheen ⁴, Siyuan Zhou ⁵ and LinShu Liu ^{1,*} 

¹ Dairy and Functional Foods Research Unit, Eastern Regional Research Center, Agricultural Research Service, United States Department of Agriculture, Wyndmoor, PA 19038, USA; jamshedbt@gmail.com (J.B.); karley.mahalak@usda.gov (K.K.M.); jenni.firman@usda.gov (J.A.F.)

² V. I. Nikitin Institute of Chemistry, National Academy of Sciences, Dushanbe 734063, Tajikistan

³ Molecular Characterization of Foodborne Pathogens Research Unit, Eastern Regional Research Center, Agricultural Research Service, United States Department of Agriculture, Wyndmoor, PA 19038, USA; yanhong.liu@usda.gov

⁴ Food Safety and Intervention Technology Research Unit, Eastern Regional Research Center, Agricultural Research Service, United States Department of Agriculture, Wyndmoor, PA 19038, USA; shiohshuh.sheen@usda.gov

⁵ Food Science College, Southwest University, Chongqing 400711, China; zhousiyuan2008@gmail.com

* Correspondence: linshu.liu@usda.gov

Abstract: Tomatoes are a perishable and seasonal fruit with a high economic impact. Carbon dioxide (CO₂), among several other reagents, is used to extend the shelf-life and preserve the quality of tomatoes during refrigeration or packaging. To obtain insight into CO₂ stress during tomato ripening, tomatoes at the late green mature stage were conditioned with one of two CO₂ delivery methods: 5% CO₂ for 14 days (T1) or 100% CO₂ for 3 h (T2). Conventional physical and chemical characterization found that CO₂ induced by either T1 or T2 delayed tomato ripening in terms of color change, firmness, and carbohydrate dissolution. However, T1 had longer-lasting effects. Furthermore, ethylene production was suppressed by CO₂ in T1, and promoted in T2. These physical observations were further evaluated via RNA-Seq analysis at the whole-genome level, including genes involved in ethylene synthesis, signal transduction, and carotenoid biosynthesis. Transcriptomics analysis revealed that the introduction of CO₂ via the T1 method downregulated genes related to fruit ripening; in contrast, T2 upregulated the gene encoding for ACS6, the enzyme responsible for S1 ethylene synthesis, even though there was a large amount of ethylene present, indicating that T1 and T2 regulate tomato ripening via different mechanisms. Quantitative real-time PCR assays (qRT-PCR) were used for validation, which substantiated the RNA-Seq data. The results of the present research provide insight into gene regulation by CO₂ during tomato ripening at the whole-genome level.

Keywords: tomato; tomato ripening; carbon dioxide; transcriptomics analysis; ethylene inhibition



Citation: Bobokalonov, J.; Liu, Y.; Mahalak, K.K.; Firman, J.A.; Sheen, S.; Zhou, S.; Liu, L. Transcriptomics Analysis of Tomato Ripening Regulated by Carbon Dioxide. *Sci* **2023**, *5*, 26. <https://doi.org/10.3390/sci5030026>

Academic Editor: Fernando Lidon

Received: 17 April 2023

Revised: 15 June 2023

Accepted: 27 June 2023

Published: 30 June 2023



Copyright: © 2023 by the authors. Licensee MDPI, Basel, Switzerland. This article is an open access article distributed under the terms and conditions of the Creative Commons Attribution (CC BY) license (<https://creativecommons.org/licenses/by/4.0/>).

1. Introduction

Tomatoes are one of the most economically important food crops, and belong to *Solanaceae* family. The dietary consumption of tomatoes is linked to many health benefits. Tomatoes contain lycopene, folate, and vitamins C and K, and are rich in minerals; it has been reported that the consumption of tomatoes can reduce the risk of heart disease and cancer [1,2]. These health benefits, coupled with their distinctive taste, make tomatoes desirable and subject to high consumer demand. However, tomatoes are a perishable, seasonal fruit. Worldwide tomato production in 2018 was more than 180 million tons (t), of which only about 1/5 were consumed without processing; the largest proportion was used for making canned tomatoes and tomato concentrates (<https://www.globenewswire.com>, accessed on 10 September 2019). Preserving the quality of fresh tomatoes and extending

their shelf-life remains a big challenge in the food industry, even though various strategies have been developed, including the use of carbon dioxide [3,4].

Ethylene is a plant hormone that regulates climacteric fruit ripening, and a number of studies have been conducted that analyze the ethylene profile during tomato ripening and its response to adverse environmental conditions like low oxygen, high temperature, etc. [3,5,6]. Among the promising technologies developed to regulate ethylene production or to maintain food quality, the use of CO₂ has attracted much attention due to its easiness to obtain, low cost [7,8], and long history of safe use for producing luscious and ripe fruits to be sold in grocery stores [9–11]. Research has found that CO₂ can either promote or inhibit ethylene production. It has been reported that the treatment of tomatoes, from the breaker to the turning stage of the ripening process, with 80% CO₂ flow for 24 h stimulated ethylene production, but delayed the color change [12]. Other reports showed that the application of 20% CO₂ flow to tomatoes at the pink stage for 24 h [13], or at the light red stage for 5 d [14], reduced ethylene production and suppressed color development. Moreover, studies on climacteric plants that used modified air with CO₂ content in the range of <1% to 100% showed that the life cycle of the tomato plant could be affected by elevated external CO₂ from the biochemical aspects of biomass synthesis, sugar signaling pathways, and hormonal crosstalk [12–16]. Based on the results of these previous studies, it is clear that the presence of CO₂ affects ethylene production and the downstream molecular mechanisms that regulate fruit growth and ripening. Yet, it is still not clear how CO₂ exerts this effect on cellular activity. The use of pure CO₂ may provide detailed information on the extent and magnitude of this effect at the molecular level.

In this study, transcriptomics was applied in order to obtain insight into the effect of CO₂ stress, under post-harvest conditions, on tomato ripening at the genomic level. Tomatoes were conditioned with gaseous CO₂ at room temperature, and their differential gene expression patterns were identified and the alteration of transcription during different developmental stages was analyzed. The application of this advanced genome analysis to elucidate the fruit ripening process at the molecular level provides a more detailed understanding of fruit ripening; in addition, this information may also be utilized to generate non-transgenic plants with improved fruit quality [17–20].

2. Materials and Methods

2.1. Tomato Fruit and CO₂ Treatment

Tomatoes (*Solanum lycopersicum* L.) in the mature green stage with uniform shapes and an average weight of 160–200 g per fruit were obtained from Coastal Sunbelt Produce, LLC (Savage, MD, USA). The tomatoes were randomly sorted into three groups. Group 1 was treated with a mixed gas (5% CO₂ and 95% air) at a flow rate of 75–100 mL/min for 14 d (T1). Group 2 was treated with 100% CO₂ gas at a flow rate of 2 L/min for 3 h (T2). Group 3 was used as a control (CT; airflow at 75–100 mL/min for 14 d). For each group, 6–7 tomatoes were loaded into an airtight jar (3.5 L) connected with a CO₂ cylinder (Air Products, Allentown, PA, USA) and an in-house air supply; gas filters, a gas mixer, and gas flow meters were used to adjusted gas composition and maintain flow rate. At each designated time point, two jars from each group were disconnected from the gas supply lines, and the tomatoes were removed and placed on a storage rack maintained at 22–24 °C and 65–75% relative humidity (RH) for subsequent physiological examination, RNA extraction, and characterization.

2.2. Characterization of Physical and Chemical Properties

Tomatoes from the T1, T2, and CT groups were examined for ethylene production, color change, firmness, and soluble carbohydrate right before treatment and on days 3, 5, 7, and 14 (d1, d3, ...).

2.2.1. Ethylene Production

A tomato from groups T1, T2, and CT of known weight was placed in an airtight jar (330 mL) on a lab bench. The sealed jar was subject to an ambient room temperature of 22–24 °C for 60 min, and then, 100 µL of gas was withdrawn from the jar using an airtight syringe and used to calculate ethylene production. The analysis was carried out on a gas chromatograph (GC) (Hewlett-Packard 5890; Hewlett-Packard, Cupertino, CA, USA) equipped with a flame ionization detector (FID) and a capillary column (30 m × 0.25 mm) coated with 5% phenyl methyl silicon (0.25 µm in thickness). Samples were injected under splitless conditions. The GC was programmed at an isothermal temperature of 30 °C, with an injection temperature of 50 °C. The detector was operated at 230 °C. Helium was used as the carrier gas at a 1.5 mL/min column flow. The amount of ethylene produced was calculated against a standard curve, which was obtained with the same instrument and operating conditions, using a known amount of ethylene gas. The production of ethylene at each time point was divided by the fruit weight and expressed as ng/g/h. Each sample was measured in triplicate.

2.2.2. Measurements of Color Change

The change in the color of the tomatoes over time was determined using images taken via photography, and also measured using a color difference meter (ColorQuest XE; HunterLab, Reston, VA, USA). The value of a^* , representing the development from the green to the red axis in the CIE color system, was used to determine surface color change during the experiment, based on an average of 20 measurements around the circumference (equatorial diameter) of each tomato.

2.2.3. Firmness Test

The firmness of the tomatoes was measured as resistance to compression using a texture analyzer (Model TA-XT2; Stable Micro System, Godalming, UK). The whole tomato was placed on a stationary steel plate with the stem end down. A 5 kg load cell was used in conjunction with a round-headed probe (P/0.25 S, $\frac{1}{4}$ spherical stainless) to compress the tomato at a crosshead speed of 3 mm/min. For each tomato, 7 separate determinations of force required to push the probe to a depth of 5 mm were obtained.

2.2.4. Total Soluble Carbohydrate Determination

The total soluble carbohydrates in the tomato juice were determined using a modified phenol–sulfuric acid method [21]. Tomato juice was centrifuged at 8700 rpm for 10 min at 22–24 °C. A fraction (0.5 mL) of the supernatant and 0.5 mL phenol solution (5%, *w/v*) were added to a round bottom glass tube (10 mL) followed by the addition of 2.5 mL of concentrated sulfuric acid. The tube was immediately capped, mixed well via vortex at the highest speed for 5 sec, and boiled for an additional 15 min. The tubes were cooled down to room temperature before reading the absorbance at 490 nm (UV-2600; Shimadzu, Columbia, MD, USA). Blank samples were prepared via the same procedure using distilled water. The carbohydrate content was calculated against a calibration curve prepared from glucose of different concentrations.

2.2.5. RNA Extraction

RNA sample preparation and sequencing were performed as previously reported [22]. Briefly, RNA samples were extracted from the pericarps of tomatoes from the T1, T2, and CT groups on days 0, 1, 3, and 7, and RNA extracted using an RNeasy Plant Mini Kit (Qiagen, Valencia, CA, USA). RNA concentrations were measured using a Nanodrop Spectrophotometer (ThermoFisher, Foster City, CA, USA). RNA purity and integrity were determined using the RNA Nano 6000 Assay Kit and an Agilent Bioanalyzer 2100 system (Agilent Technologies, Santa Clara, CA, USA) with an RNA integrity number (RIN) between 9.0 and 9.7 for all samples.

2.3. RNA-Seq and Data Analysis

RNA sequencing and subsequent bioinformatic analysis were performed by Novogene Bioinformatics Technology Co., Ltd. (Beijing, China). Sequencing libraries were constructed using 3 µg of RNA per sample with the NEBNext Ultra RNA Library Prep Kit and quantified using a Qubit 2.0 fluorimeter. The insert sizes were determined using an Agilent 2100 Bioanalyzer. The library preparations were then sequenced on an Illumina Sequencing System (Illumina HiSeq 2000; Illumina, San Diego, CA, USA) and 150 bp paired-end reads were generated. Each sample treatment (T1, T2, and CT groups) was sequenced in duplicate.

After filtering low-quality reads from the raw data, clean reads with a quality score over Q20 were mapped against the *S. Lycopersicum* genome using TopHat v2.0.12 software. Gene expression levels were determined based on reads per kilobase million (RPKM) of mapped reads. Genes with q -values < 0.05 were considered differentially expressed genes (DEGs). The comparison of DEGs between different groups was carried out using the DESeq R package. The DEGs were used for Gene Ontology (GO) (Version 2.12.) analysis and Kyoto Encyclopedia of Genes and Genomes (KEGG) (V2.0) enrichment analysis using the KOBAS software.

2.4. Real-Time Quantitative Reverse Transcription Polymerase Chain Reaction (qRT-PCR) Assays

The synthesis of cDNA was performed using an Applied Biosystems GeneAmp PCR System 9700 (ThermoFisher, Foster City, CA, USA) as described previously [22]. Primers designed using Primer3 (v.0.4.0) software based on the gene sequences are listed in Supplementary Table S1.

2.5. Statistical Analysis

The Student's t -test was used to determine whether there were significant difference between samples for all measurements.

3. Results

3.1. Changes in the Phenotypes of Tomatoes Induced by Carbon Dioxide

The ethylene production of tomatoes at the beginning of the experiment, d0, was ~2 ng/g/h for all groups (Figure 1a), indicating that all the tomatoes were in the MG3 growth stage, or the late stage of mature green [23,24]. In the control group (CT), ethylene production stayed at 2 ng/g/h for the first 3 days and was followed by a sharp increase during the following 4 days, reached peak levels on d7, and then, gradually decreased to a constant level by d14; the color of the tomatoes in the CT group turned to orange-pink by d3 (Figure 1b), and became totally red by d7. In comparison with the CT group, significant inhibition of ethylene synthesis occurred for tomatoes in the T1 group throughout the whole experiment (Figure 1a). The examined tomatoes before treatment appeared green in color; the shade of green varied from light to dark (Figure 1b). The tomatoes in the T1 group maintained their green color for 7 days (Figure 1b), and then, remained pink until the experiment was terminated. The differences in the ethylene production and color development between groups CT and T1 were closely associated with the changes in a^* values (Figure 1c), firmness (Figure 1d), and soluble carbohydrates (Figure 1e).

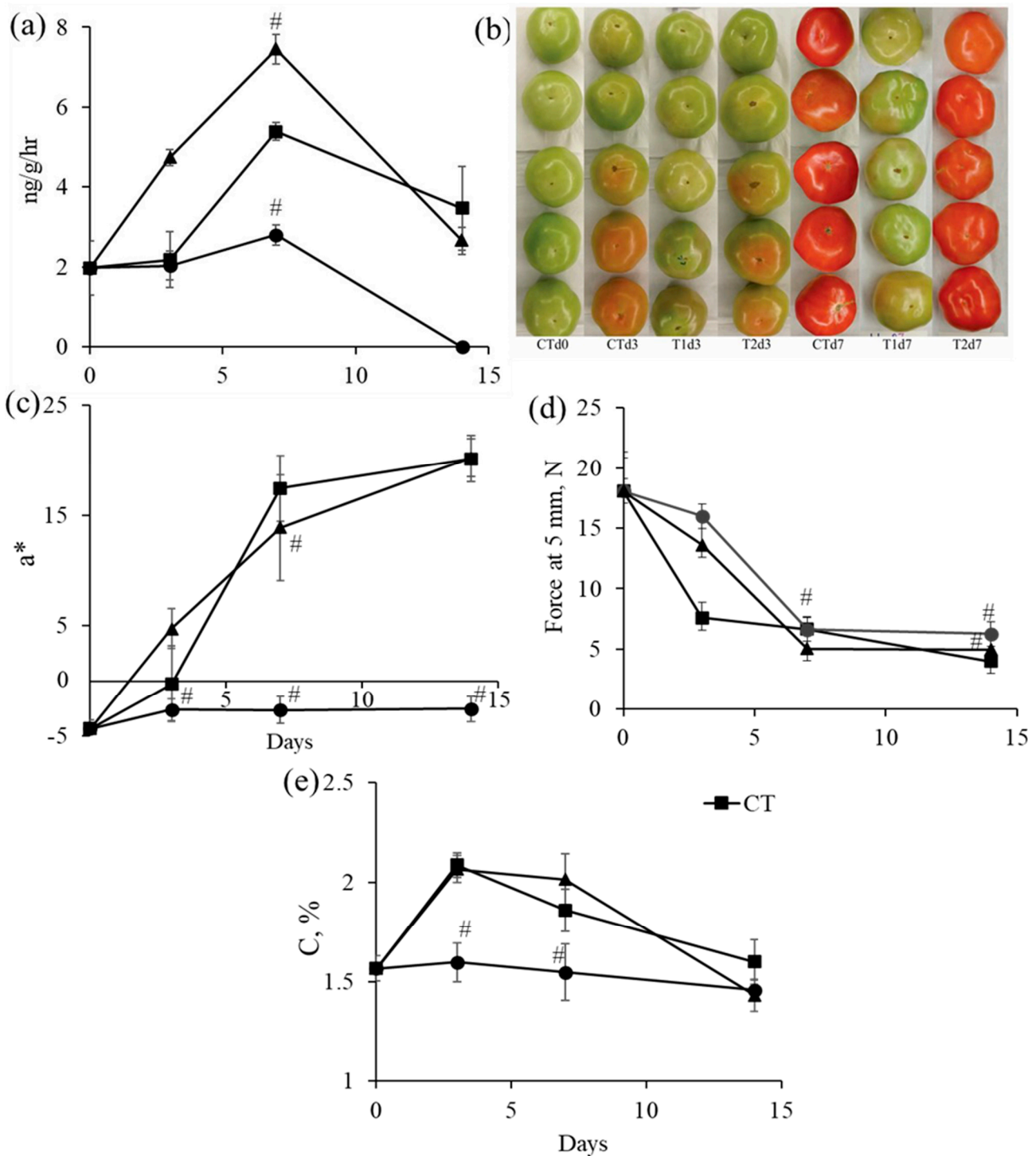


Figure 1. Changes in phenotypes induced by exogenous CO₂. (a) Ethylene production; (b) photos of tomatoes; (c) a* values; (d) firmness; and (e) soluble carbohydrates. Error bars indicate the standard deviation of three replications. (■) CT, (●) T1, (▲) T2; # *p* < 0.05 (Student’s *t*-test).

In contrast to the T1 group, the measured ethylene production of the T2 group was about 2.5 and 1.4 times that of CT on d3 and d7, respectively. The ethylene production of the T2 group gradually decreased thereafter, approaching levels similar to those of the CT group on d14 (Figure 1a). The color of the T2 group tomatoes turned from green to slightly pink by d3 but became as red as the CT group tomatoes by d7 (Figure 1b). The measurements of CIE color value and firmness in the T2 group were higher than in the

CT group on d3, and the differences in the a* value and firmness of the tomatoes between groups T2 and CT became negligible by d7 (Figure 1c,d). Furthermore, both T2 and CT tomatoes had similar extraction curves for soluble carbohydrates (Figure 1e).

The two CO₂ delivery methods had opposite effects on ethylene production, yet they had the same trends for other components of tomato ripening (color change, firmness, soluble carbohydrate). In this context, the genes encoding for ethylene biosynthesis and signal processing, for differentiation from chloroplast to chromoplast, and for cell-wall degradation are discussed in the following sections.

3.2. Transcriptome and Bioinformatics Analysis

Total RNA was extracted from the pericarps of tomatoes in groups T1, T2, and CT on days 3 and 7 after treatment. These time points were selected because they demonstrated the largest differences in ethylene production between T1, T2, and CT. RNA-Seq generated 62.7–92.8 million reads for each sample, with a quality score of $\geq Q20$ for 97% of the raw reads. Clean reads ranging from 60.1 to 89.2 million per sample were obtained after filtering. Approximately 53–82% of clean reads could be mapped to the tomato reference genome (Table 1). Uniquely mapped reads comprised more than 53% of the total clean reads, and multiple-mapped reads accounted for less than 0.8%, indicating that the sequencing results were relatively stable. The uniquely mapped RNA-Seq data were used to analyze changes in the cellular transcriptome induced by CO₂.

Table 1. Throughput and quality of RNA sequencing data.

Sample Name *	Raw Reads	Clean Reads	Q20 ** (%)	Total Mapped	Multiple-Mapped	Uniquely Mapped
CTd3 1	65,773,470	63,817,890	97.28	51,738,379 (81.07%)	454,994 (0.71%)	51,283,385 (80.36%)
CTd3 2	73,676,038	71,179,598	97.14	57,513,775 (80.8%)	581,015 (0.82%)	56,932,760 (79.98%)
CTd7 1	64,366,640	61,793,974	96.93	35,012,094 (56.66%)	256,136 (0.41%)	34,755,958 (56.24%)
CTd7 2	62,739,824	60,506,740	97.14	32,240,221 (53.28%)	244,883 −0.40%	31,995,338 (52.88%)
T1d3 1	82,567,552	79,299,482	97.06	58,963,542 (74.36%)	461,800 (0.58%)	58,501,742 (73.77%)
T1d3 2	64,498,224	62,077,256	96.97	51,142,314 (82.38%)	375,820 (0.61%)	50,766,494 (81.78%)
T1d7 1	90,148,126	86,721,258	97.16	64,317,498 (74.17%)	518,547 −0.60%	63,798,951 (73.57%)
T1d7 2	92,821,490	89,213,582	97.04	57,915,789 (64.92%)	458,066 (0.51%)	57,457,723 (64.4%)
T2d3 1	74,724,698	72,157,326	97.23	51,476,059 (71.34%)	325,579 (0.45%)	51,150,480 (70.89%)
T2d3 2	76,499,736	74,025,794	97.24	45,151,183 (60.99%)	283,328 (0.38%)	44,867,855 (60.61%)
T2d7 1	73,727,656	70,981,232	97.09	38,103,699 (53.68%)	266,548 (0.38%)	37,837,151 (53.31%)
T2d7 2	70,278,582	67,611,036	96.99	49,525,905 (73.25%)	354,644 (0.52%)	49,171,261 (72.73%)

* Sample names, combining the letter and number of “d3” and “d7” after the group name (CT, T1, or T2) in this Table and throughout all Tables and Figures and the text, indicate the sampling day after treatment. For example, “T1d3” denotes samples that were taken from the T1 group on day 3 after CO₂ treatment, and the suffix (1 or 2) is the testing number; ** Q20 is a quality score indicating that the probability of an incorrect base call is 1 in 100.

A significant number of genes from groups T1, T2, and CT with different abundances were detected. Among them, approximately 50% contained fragments per kilobase million (FPKM) ≥ 1 . The variations in the significantly differentially expressed genes (DEGs) from groups T1, T2, and CT on d3 (T1d3, T2d3, and CTd3) and d7 (T1d7, T2d7, and CTd7) are shown in Figure 2. In comparison with CTd3, 3181 DEGs were significantly upregulated and 3943 were downregulated in T1d3 (Figure 2a); 3425 DEGs were significantly upregulated and 3616 were downregulated in the T2d3 group (Figure 2b). When compared to CTd7, T1d7 contained 4110 upregulated DEGs and 4187 downregulated (Figure 2c), while only 312 DEGs were upregulated and 293 downregulated in T2d7 (Figure 2d). In comparison to T1d7 to T2d7, there were 4383 upregulated genes and 4266 downregulated (Supplementary Figure S1). These results indicate that both methods of CO₂ treatment, either with continuous 5% CO₂ flow for the entire experiment (T1) or with nearly 100% gaseous CO₂ for only 3 h (T2), are able to modulate gene expression in treated tomatoes; however, the T1 method has a stronger and more long-term influence on measurable, physical characteristics compared to T2.

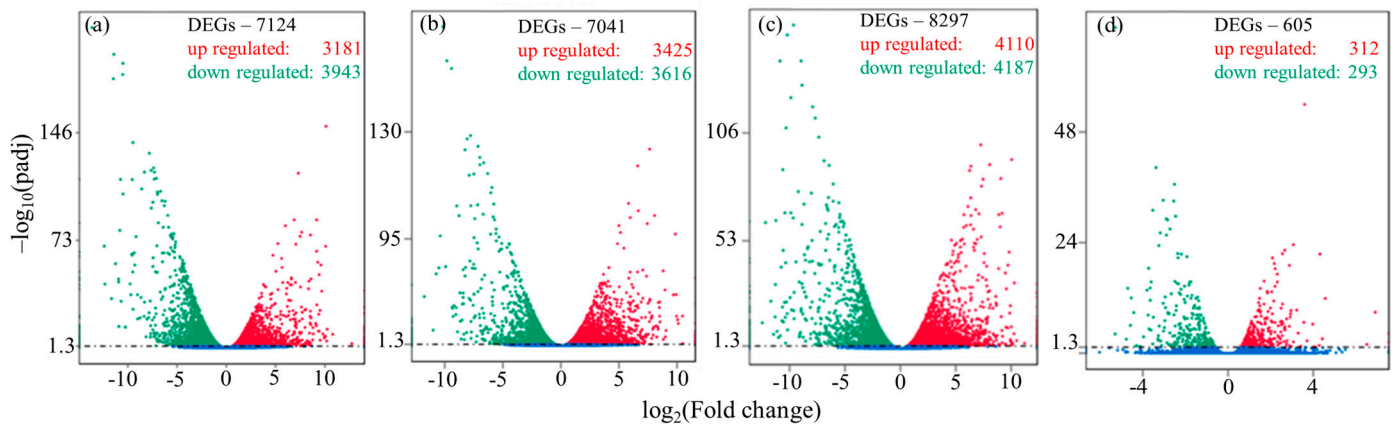


Figure 2. Volcano plot of significant DEG numbers of CO₂ treated tomatoes on (a) T1d3:CTd3; (b) T2d3:CTd3; (c) T1d7:CTd7; and (d) T2d7:CTd7.

Next, all identified DEGs were clustered using hierarchical analysis, and the overall results are summarized in Figure 3. In the heatmap, red and blue colors represent genes with higher and lower expression levels, respectively; the color transition from red to blue indicates a change in gene expression from a high to a low level. The expression levels for the identified DEGs in T2 and CT display a more similar pattern on d7 than d3. This indicates that the administration of CO₂ had only a transient effect on gene expression for the T2 group, and the levels returned to those similar to the control by day 7 post-exposure. This observation is supported by the results in Figure 1. Conversely, the pattern of gene expression for both T1d3 and T1d7 is highly divergent from CTd3 and CTd7, indicating that differential expression between these groups occurred after exposure and was maintained until the end of the experiment. These results match the ethylene production profile depicted in Figure 1.

Next, bioinformatics analysis was applied to cluster the functional genes into different bioprocesses using Gene Ontology (GO) and the KEGG pathway. The distribution of DEGs into biological processes (BP), cellular components (CC), and molecular function (MF) were investigated via GO analysis. A total of 10 BP terms and 20 CC terms in T1d7:CTd7 (Figure 4a), as well as 4 BP terms and 2 MF terms in T2d7:CTd7 (Figure 4b), were significantly enriched, suggesting that these genes are most strongly regulated by CO₂ application. Consequently, when T1 was compared to T2 on day 7, 8 BP terms and 22 CC terms were significantly enhanced (Supplementary Figure S2). KEGG analysis showed that the biosynthesis of amino acids and pyruvate metabolism in the two comparison groups of “T1d7:CTd7” and “T1d7:T2d7” were among the most significantly enriched pathways ($p < 0.05$ and $q < 0.05$). Beta-alanine metabolism in “T1d7:CTd7”, second metabolite and flavonoid biosynthesis, and plant–pathogen interaction pathways in “T2d7:CTd7”, as well as the glycolysis/gluconeogenesis pathway in “T1d7:T2d7”, were also significantly influenced ($p < 0.05$ and $q < 0.05$; Figure 4c,d, and Supplementary Figure S3).

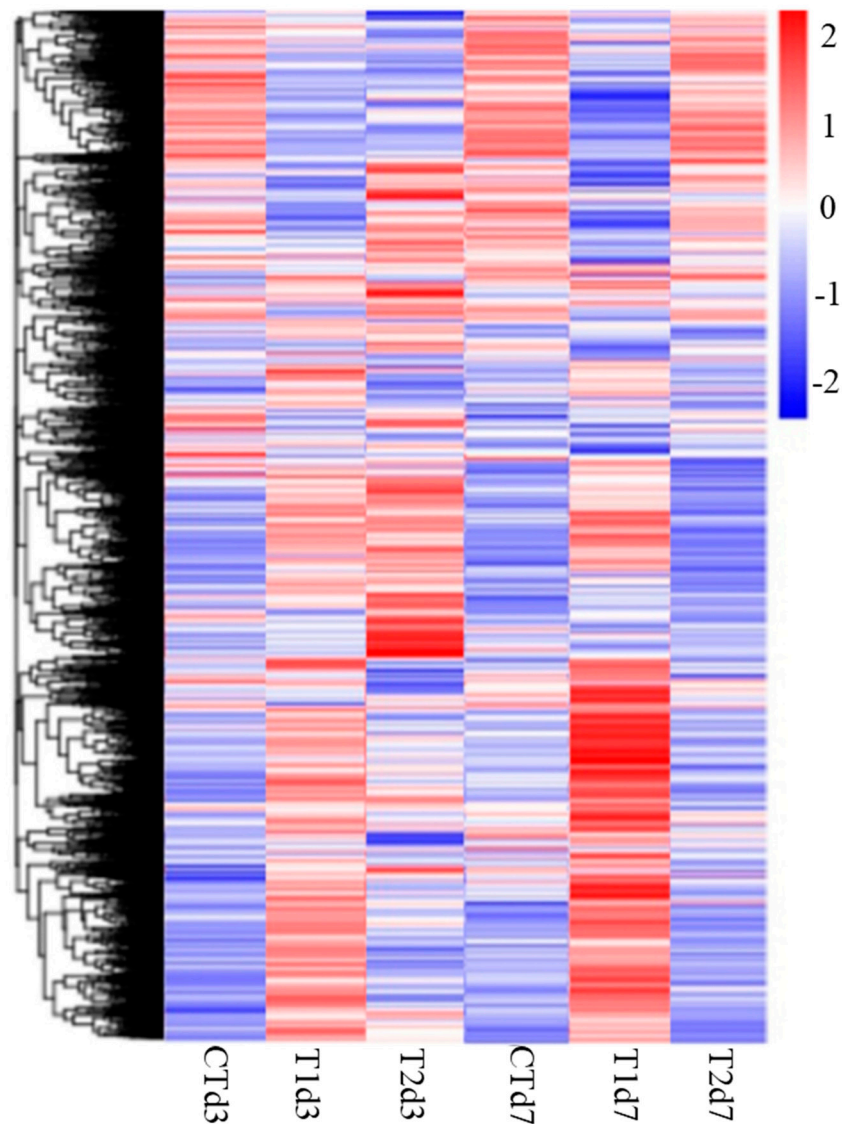


Figure 3. Hierarchical clustering and heat map of expression levels of differentially expressed genes in RPKM. In the heat map, red is associated with high expression levels, and blue is associated with low expression levels. Data represented are the averages of two biological replicates.

3.3. DEGs Encoding for Ethylene Synthesis and Signal Transduction

Previous results [12–14] have indicated that the effects of CO₂ on tomato ripening are related to ethylene production. In the present study, 39 genes that were differentially expressed in response to CO₂ treatment and involved in ethylene synthesis and signal transduction were evaluated. Four genes encoding for methionine adenosyltransferase synthesis (Solyc10g083970, Solyc09g008280, Solyc12g099000, and Solyc01g101060) were regulated by CO₂ treatments (Table 2). The gene encoding for S-adenosylmethionine synthase 2 was upregulated by both T1 and T2 treatments on day 3; however, for the T2 group, the level of expression returned to normal, while for the T1 group, the level of expression remained significantly upregulated on day 7. The most noticeable difference in the gene expression of S-adenosylmethionine synthase between T1 and T2 was for the gene Solyc09g008280, which was inhibited in the T1 group yet significantly upregulated on d7 for the T2 group (T2d7:CTd7). The expression level of the gene Solyc01g101060 encoding for S-adenosylmethionine synthase 1 was statistically enhanced by T2 on d3, while it was downregulated on d7 by both T1 and T2 treatment.

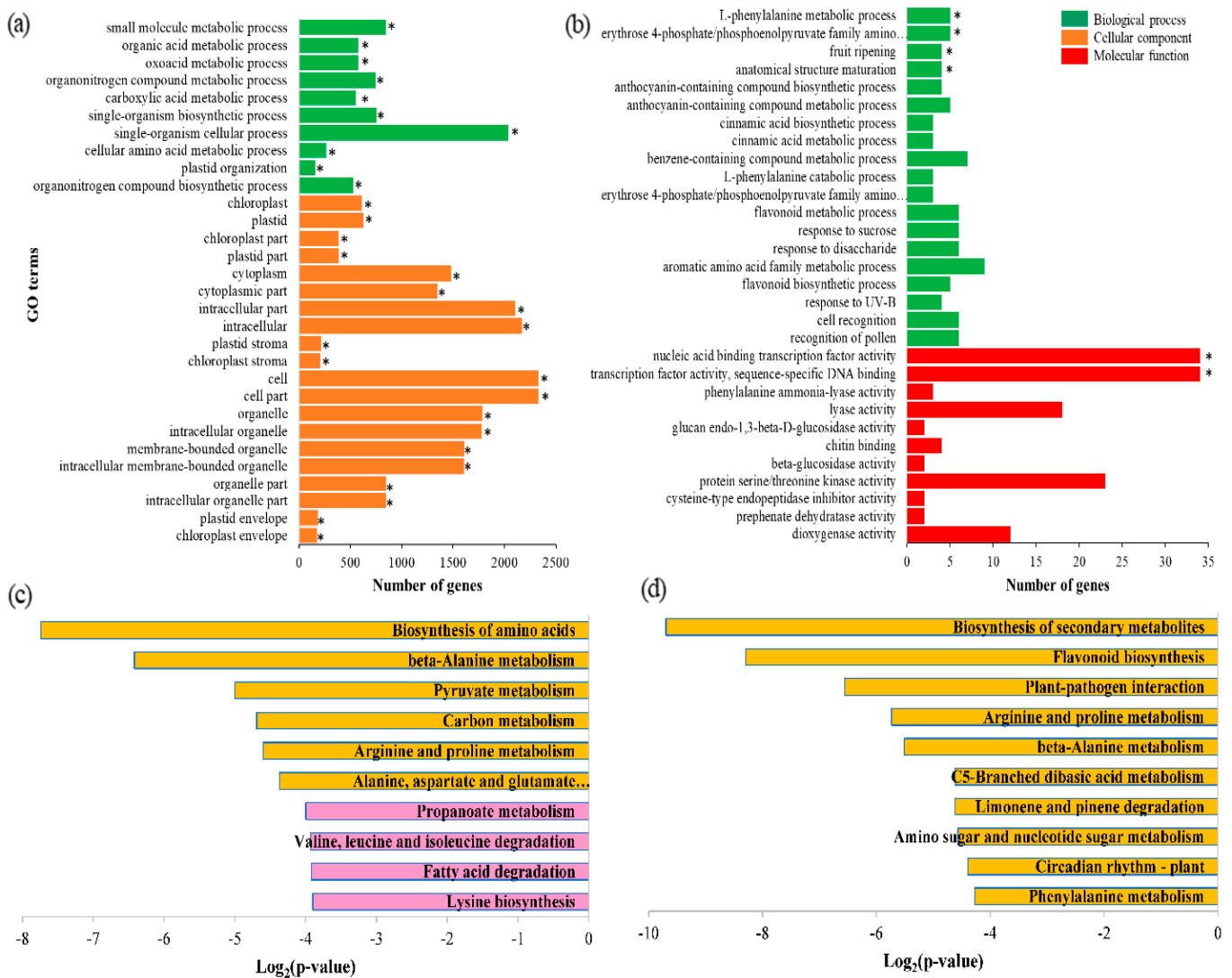


Figure 4. Gene Ontology (GO) and KEGG pathway enrichment analysis of DEGs on d7. (a) The most enriched GO terms in T1:CT; (b) the most enriched GO terms in T2:CT; (c) KEGG analysis in T1:CT; (d) KEGG analysis in T2:CT. In (a,b), bars with asterisks (*) indicate $q < 0.05$. In (c,d), for all bars, $q < 0.05$ and $p < 0.05$, except for pink bars, for which $p > 0.05$.

Six genes encoding for 1-aminocyclopropane-1-carboxylate synthase (ACS) and another six genes encoding for 1-aminocyclopropane-1-carboxylate oxidase (ACO) were found to be differentially expressed among the samples. Out of the 48 samples examined, 43 exhibited downregulation of ACS and ACO, indicating the inhibitive effect of CO₂ on ethylene production. However, five samples displayed an increase in expression. The highest increase was for the ACO gene Solyc02g081190, which was significantly upregulated by T1 and T2 treatments on day 3 by 21.22% and 73.99%, respectively. For the T1 group, this remained significantly enhanced by day 7, but for the T2 group, expression was not detected on day 7. Additionally, the ACS gene Solyc01g095080 was significantly upregulated by T2 treatment on d7. The differential expression of the gene Solyc08g008100 for T2 was statistically higher on d3 compared to the control (Figure 5, Table 2).

Table 2. DEGs involved in ethylene synthesis (fold change).

Gene ID	Annotation	T1d3:CTd3	T2d3:CTd3	T1d7:CTd7	T2d7:CTd7
Solyc10g083970	S-adenosylmethionine synthase	-	-	-	-
Solyc09g008280	S-adenosylmethionine synthase 3	-	-	-	4.02
Solyc12g099000	S-adenosylmethionine synthase 2	3.83	3.73	2.11	-
Solyc01g101060	S-adenosylmethionine synthase 1	-	3.21	0.32	0.65
Solyc08g008110	1-aminocyclopropane-1-carboxylate synthase	0.13	-	-	-
Solyc08g008100	1-aminocyclopropane-1-carboxylate synthase 6	0.34	5.2	-	-
Solyc05g050010	1-aminocyclopropane-1-carboxylate synthase 4	0.01	0.01	0	-
Solyc01g095080	1-aminocyclopropane-1-carboxylate synthase 2	-	0.09	-	2.79
Solyc08g081550	1-aminocyclopropane-1-carboxylate synthase 1a	-	-	0.29	-
Solyc08g081540	1-aminocyclopropane-1-carboxylate synthase 1b	0.2	-	-	-
Solyc07g049530	1-aminocyclopropane-1-carboxylate oxidase 1	0.38	0.31	0.49	-
Solyc09g089580	1-aminocyclopropane-1-carboxylate oxidase-like protein	0.07	0.01	0.07	-
Solyc02g081190	1-aminocyclopropane-1-carboxylate oxidase 4	21.22	73.99	8.96	-
Solyc07g049550	1-aminocyclopropane-1-carboxylate oxidase	0.12	0.03	0.31	0.29
Solyc07g026650	1-aminocyclopropane-1-carboxylate oxidase 5	0.05	-	0.17	-
Solyc02g036350	1-aminocyclopropane-1-carboxylate oxidase	0.14	-	0.07	-
Solyc09g089580	1-aminocyclopropane-1-carboxylate oxidase-like protein	0.07	0.01	0.07	-

All data shown in this table are statistically significant; “-” indicates statistically non-significant.

Ethylene signal transduction is another important element in regulating the biochemical processes initiated by ethylene binding. Compared to the CT group, the expression levels of the genes Solyc05g055070 (ethylene receptor), Solyc09g075440 (never ripe), Solyc07g008250 (EIN3-, F-box protein), and Solyc12g009560 (EIN3-binding F-box protein 1) were dramatically downregulated on d3 for the T1 group; in addition to these four genes, Solyc09g007870 (Ethylene insensitive 2) was also downregulated on d7. Compared to the CT group on d3, three genes were suppressed in the T2 group, including Solyc09g075440 (never ripe); six genes were significantly upregulated, including Solyc09g007870 (ethylene insensitive 2) and Solyc12g009560 (EIN3-binding F-box protein 1), both of which interact with EBF1 and -2 and are considered transcriptional regulators that are important for ethylene signaling [25]. The ripening of T2 tomatoes occurred over time, and by d7, no significant differences between T2 and CT could be detected, except for the three genes encoding for ethylene response factors a2, c6, and e3, which were significantly downregulated in T2 (Figure 5, Table 3).

One critical element that influences signal transduction is DNA methylation [26–30]. There were nine genes involved in epigenetic modification detected in this experiment, with six genes encoding for DNA methyltransferase and three genes for DNA demethylase (Table 4). Compared to the CT group, two DNA demethylase-encoding genes, Solyc10g083630 and Solyc11g007580, were downregulated in the T1 group on d3 and d7, and in the T2 group on d3 only. In addition, a cytosine-5 DNA methyltransferase gene, Solyc02g062740, was found to be downregulated in the comparison groups “T1:CT” and “T2:CT” on d3 and d7, but the decrease was statistically significant only for tomatoes treated with the T1 method. Two DNA methyltransferase genes, Solyc11g030600 and Solyc12g100330, were upregulated in the comparison group “T1d3:CTd3”. Interestingly, no significant differences in DNA methylation/demethylation were detected between T2 and CT on d7.

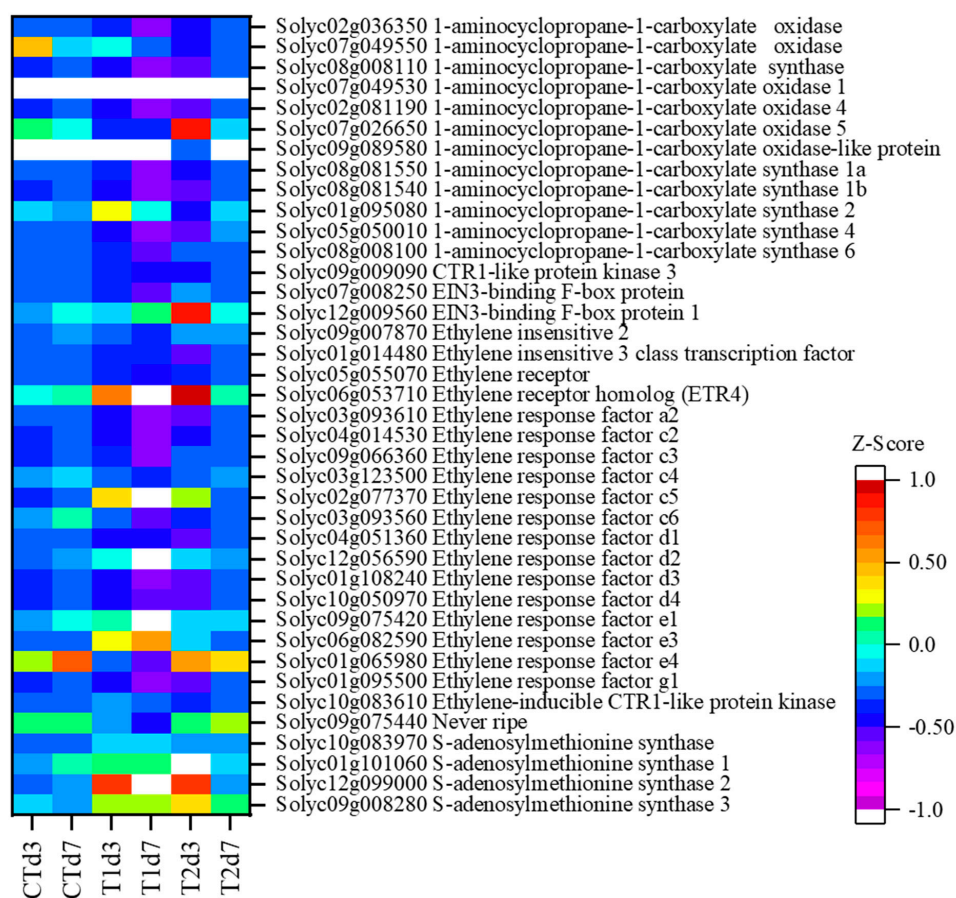


Figure 5. Heat map depicting expression levels of DEGs involved in ethylene synthesis and signal transduction. Red indicates high expression, while blue denotes low expression. The RPKM values were normalized with $\log_2(\text{RPKM} + 1)$ and converted to Z-scores.

Table 3. Genes involved in ethylene signal transduction (fold change).

Gene ID	Annotation	T1d3:CTd3	T2d3:CTd3	T1d7:CTd7	T2d7:CTd7
Solyc05g055070	Ethylene receptor	0.4	-	0.52	-
Solyc06g053710	Ethylene receptor homolog (ETR4)	-	-	-	-
Solyc09g075440	Never ripe	0.11	0.33	0.06	-
Solyc09g009090	CTR1-like protein kinase 3	-	-	-	-
Solyc10g083610	Ethylene-inducible CTR1-like protein kinase	-	-	-	-
Solyc09g007870	Ethylene insensitive 2	-	1.58	0.52	-
Solyc01g014480	Ethylene insensitive 3 class transcription factor	-	-	1.91	-
Solyc07g008250	EIN3-binding F-box protein	0.37	-	0.24	-
Solyc12g009560	EIN3-binding F-box protein 1	0.62	2.31	0.42	-
Solyc01g095500	Ethylene response factor g1	-	-	-	-
Solyc01g065980	Ethylene response factor e4	0.05	0.43	0.02	-
Solyc06g082590	Ethylene response factor e3	7.82	4.23	13.31	0.39
Solyc09g075420	Ethylene response factor e1	-	0.54	-	-
Solyc10g050970	Ethylene response factor d4	0.14	-	145.91	-
Solyc01g108240	Ethylene response factor d3	-	-	-	-
Solyc12g056590	Ethylene response factor d2	-	1.66	5.67	-
Solyc04g051360	Ethylene response factor d1	0.27	-	17.94	-
Solyc03g093560	Ethylene response factor c6	0.19	0.38	0.04	0.1
Solyc02g077370	Ethylene response factor c5	43.87	37.77	128.16	-
Solyc03g123500	Ethylene response factor c4	0.36	0.53	0.26	-
Solyc09g066360	Ethylene response factor c3	7.58	87.66	-	-
Solyc04g014530	Ethylene response factor c2	-	-	-	-
Solyc03g093610	Ethylene response factor a2	0.13	-	0.26	0.24

All data shown in this table are statistically significant; “-” indicates statistically non-significant.

Table 4. DEGs associated with DNA methylation (fold change).

Gene ID	Annotation	T1d3:CTd3	T2d3:CTd3	T1d7:CTd7	T2d7:CTd7
Solyc11g030600	DNA (Cytosine-5)-methyltransferase	1.68	1.69	-	0.61
Solyc12g100330	Cytosine-specific methyltransferase	1.93	0.69	1.87	-
Solyc08g005400	Cytosine-specific methyltransferase	-	-	3.19	-
Solyc02g062740	DNA (Cytosine-5)-methyltransferase 3	0.59	-	0.63	-
Solyc10g078190	DNA (Cytosine-5)-methyltransferase 3	-	-	2.15	-
Solyc04g005250	DNA (Cytosine-5)-methyltransferase 3	-	-	-	-
Solyc09g009080	Repressor of silencing 1	-	2.27	3.1	-
Solyc10g083630	Repressor of silencing 2b	0.06	0.25	0.05	-
Solyc11g007580	HhH-GPD family protein	0.24	0.74	0.31	-

All data shown in this table are statistically significant; “-” indicates statistically non-significant.

3.4. DEGs Encoding for Color Change and Cell-Wall Degradation

Table 5 shows the genes identified that were involved in lycopene synthesis in response to exogenous CO₂. The genes Solyc01g097810 (zeta-carotene desaturase), Solyc03g031860 (phytoene synthase 1), and Solyc02g081330 (phytoene synthase 2) were downregulated in the T1 group throughout the experiment, while a decrease in these genes’ expression was only detected on d3 for the T2 group.

Table 5. DEGs associated with carotenoid metabolism (fold change).

Gene ID	Annotation	T1d3:CTd3	T2d3:CTd3	T1d7:CTd7	T2d7:CTd7
Solyc02g090890	Zeaxanthin epoxidase	6.63	16.54	0.46	-
Solyc01g097810	Zeta-carotene desaturase	0.21	0.26	0.15	-
Solyc02g081330	Phytoene synthase 2	0.29	-	0.19	-
Solyc03g031860	Phytoene synthase 1	0.05	0.05	0.01	-
Solyc10g079480	Beta-lycopene cyclase	-	16.09	61.63	-
Solyc04g040190	Lycopene beta-cyclase	0.21	-	0.12	-
Solyc06g074240	Lycopene beta cyclase	0.14	0.05	-	-
Solyc10g083790	Cytochrome P450	-	-	-	-
Solyc10g081650	Carotenoid isomerase	0.1	0.28	0.08	-
Solyc03g007960	Beta-carotene hydroxylase-2	0.07	0.07	0.01	-
Solyc01g009230	Xanthine dehydrogenase/oxidase	2.76	2.37	-	0.48
Solyc01g108210	Cytochrome P450	6.52	5.71	-	-
Solyc03g123760	Phytoene desaturase	0.11	0.3	0.08	-
Solyc04g050930	Violaxanthin de-epoxidase	0.06	0.22	0.06	-
Solyc04g051190	Cytochrome P450	-	-	-	-
Solyc04g071940	Xanthoxin dehydrogenase	0.5	0.48	0.29	-

All data shown in this table are statistically significant; “-” indicates statistically non-significant.

It was also found that expression of the zeaxanthin epoxidase encoding-gene (Solyc02g090890) was significantly upregulated on d3 but suppressed on d7 in both groups T1 and T2. Lycopene beta-cyclase genes (Solyc04g040190 and Solyc06g074240), carotenoid isomerase (Solyc10g081650), and beta-carotene hydroxylase-2 (Solyc03g007960) were downregulated in the comparison group “T1:CT” on both d3 and d7, whereas a gene encoding for beta-lycopene cyclase (Solyc10g079480) was upregulated. In the comparison group “T2d7:CTd7”, no statistically significant differences were detected for most of these genes. Genes encoding for xanthine dehydrogenase/oxidase (Solyc01g009230) and cytochrome P450 (solyc01g108210) were upregulated on d3 in both comparison groups “T1:CT” and “T2:CT”.

A set of genes related to polysaccharide synthesis and association have been demonstrated to be crucially important for cell-wall degradation, including those encoding for polygalacturonase (Solyc10g080210 and Solyc06g060170), pectinesterase (Solyc03g083360 and Solyc07g017600), beta-xylosidase (Solyc01g104950, Solyc02g091680, and Solyc10g047030), pectate lyase (Solyc03g111690 and Solyc09g091430), and expansin (Solyc06g051800 and Solyc10g086520). All these genes were statistically downregulated in both the comparison groups “T1d3:CTd3” and T1d7:CTd7” (Table 6). Among these genes, the expression levels of Solyc03g083360, Solyc02g091680, Solyc09g091430, and Solyc06g051800 were significantly

decreased. The decrease in the transcription of these genes in the T1 group supports the findings in Figure 1, where tomatoes in the T1 group remained green and were significantly firmer compared to the control.

Table 6. DEGs associated with cell-wall degradation (fold change).

Gene ID	Annotation	T1d3:CTd3	T2d3:CTd3	T1d7:CTd7	T2d7:CTd7
Solyc10g080210	Polygalacturonase-2 precursor	0	0	0	2.22
Solyc06g060170	Probable polygalacturonase-like	-	-	-	-
Solyc12g098340	Probable pectinesterase 29-like	-	-	-	-
Solyc03g083360	Probable pectinesterase	0.13	0.52	-	-
Solyc03g078090	Probable pectinesterase	-	-	-	-
Solyc07g017600	Pectinesterase	0.03	-	-	-
Solyc09g010210	Endo-1,4-beta-glucanase precursor	0.01	-	0	-
Solyc02g091680	Probable beta-D-xylosidase 6-like	0.3	0.47	0.32	-
Solyc01g104950	Beta-xylosidase	0.27	-	-	-
Solyc10g047030	Beta-D-xylosidase 1 precursor	0	-	0.01	-
Solyc09g005850	Probable pectate lyase 4-like	-	-	-	2.09
Solyc03g111690	Probable pectate lyase 18-like	0	0.02	0	-
Solyc09g091430	Probable pectate lyase 15-like	0.01	0.33	0.01	5.85
Solyc03g031840	Expansin precursor	-	11.81	-	-
Solyc06g051800	Expansin 1	0.09	0.13	0	-
Solyc10g086520	Expansin precursor 6	0.22	0.18	-	-
Solyc02g088100	Expansin precursor 5	-	14.93	-	-

All data shown in this table are statistically significant; “-” indicates statistically non-significant.

3.5. DEGs Encoding for Stress Resistance Induced by CO₂ Treatment

The DEGs involved in the stress response pathways are listed in Figure 6. In the heatmap, the samples (in rows) and genes (in columns) are both hierarchically clustered so that genes with more similar transcription patterns are adjacent, and so are the samples. What we can see clearly here is that tomatoes treated with the T1 method are the most distinct. The T2 samples at timepoint d7 are similar to the control samples, and the T2 samples from timepoint d3 are more similar to the T1 samples, but still different. The results are also shown in Supplementary Table S2. The genes encoding for enzymes offering resistance to stress include heat shock proteins (Solyc07g047790 and Solyc08g078700), a late embryogenesis-abundant protein (Solyc09g008770), amino oxidase family proteins (Solyc07g043590 and Solyc02g081390), dehydrin DHN1 (Solyc02g084840), glutaredoxin (Solyc09g005620), zeaxanthin epoxidase (Solyc02g090890), and homeobox protein (Solyc07g007120). These genes are not only induced by CO₂, but are also stimulated by heat, light, drought, and other abiotic and biotic stress, thereby playing a key role in acclimation to environmental stress conditions [31–33].

CO₂ stress also introduced changes in expression for genes encoding various distinct functions, such as Solyc02g088630, which is a glycotransferase that participates in oligo-/poly-saccharides and glycoconjugate biosynthesis, and regulates functions from structure and storage to signaling; Solyc02g089540, which plays a key role in controlling flower time; and Solyc02g086670, which has a significant role in cellular processes, especially in phosphorylation. The genes Solyc08g082210 and Solyc02g091700 are also involved in the disease resistance pathway. Differential expression of a group of genes that directly responded to the fruit ripening process was also found to be regulated by CO₂ stress. These include genes such as Solyc02g081330, which plays a role in the biosynthesis of carotenoids; Solyc02g090890, which is involved in carotenoid degradation; Solyc08g079180, which codes for protein translocation and cell-wall stability; Solyc02g091700, which codes for a cell-wall component and plays a role in cell shape; Solyc02g087060, which is an integral component of the cell membrane; and Solyc08g082210, which is part of the ethylene signaling pathway.

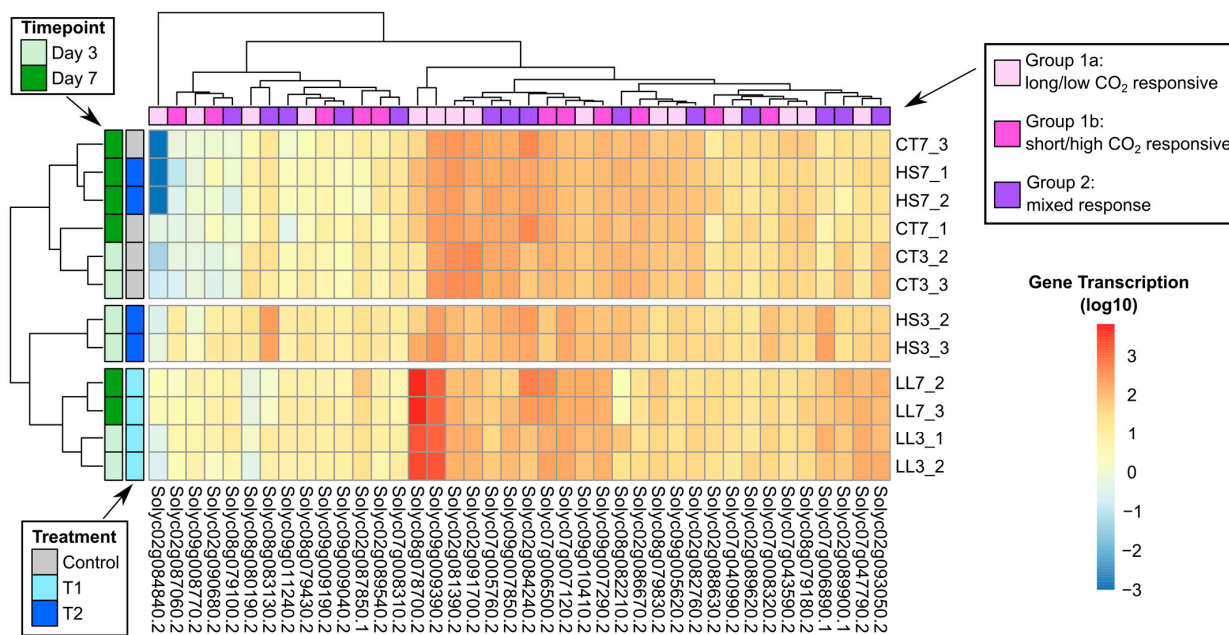


Figure 6. Heatmap of the expression levels of the DEGs induced by CO₂ stress. Genes in columns with more transcription patterns are adjacent; samples in rows of more transcription patterns are also adjacent.

3.6. Correlation of Gene Expression Data from RNA-Seq and qRT-PCR

qRT-PCR was used to validate the RNA-Seq data. From the results of the transcriptomics analysis of the comparison groups “T1:CT”, “T2:CT”, and “T1:T2” on d7, 10 genes with different levels of expression were randomly selected from each group for a RT-PCR assay. This assay illustrated a similar expression pattern between the two analytical methods with an acceptable correlation coefficient of R², falling between 0.84 and 0.88, indicating the reliability of the RNA-Seq results. Figure 7 shows that the gene expression data obtained from RNA-Seq correlated very well with the qRT-PCR assay.

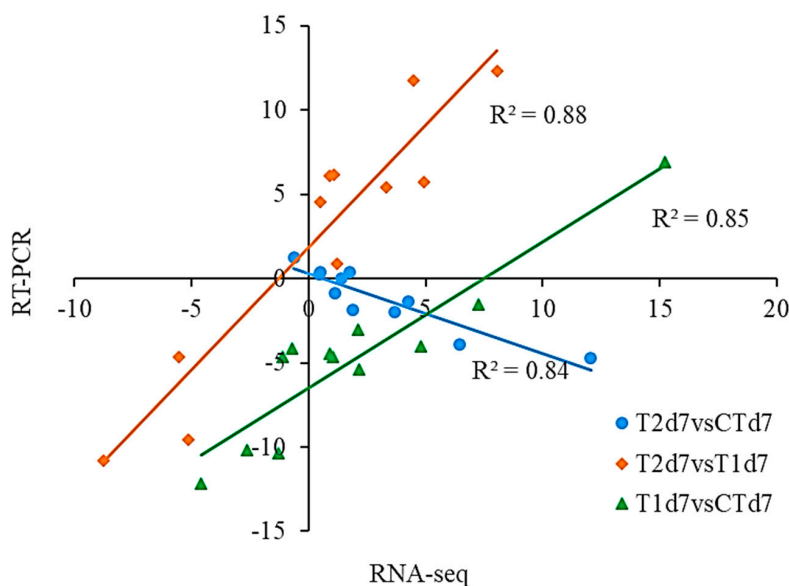


Figure 7. Correlation of gene expression data from RNA-Seq and RT-qPCR: (triangle) T1d7:CTd7; (circle) T2d7:CTd7; (diamond) T2d7:T1d7.

4. Discussion

Tomatoes are climacteric fruits characterized by a surge in ethylene biosynthesis at the onset of ripening. Tomato ripening occurs due to the activation of a series of molecular pathways that determine changes in appearance and nutrition, pigmentation levels, the production of volatiles, sweetness and acidity, and the promotion of tissue softening [34–36]. Figure 8 illustrates the current understanding of the correlation between ethylene biosynthesis during a tomato’s growth and ripening and its morphophysiological steps. System 1 (S1, auto-inhibitory) is responsible for producing basal ethylene levels during fruit growth, while system 2 (S2, auto-catalytic) operates during climacteric ripening. The pathway of ethylene biosynthesis in both S1 and S2 can be simplified into 3 steps: Step I, Methionine (precursor) → S-adenosylmethionine (intermediate, SAM); Step II, SAM → 1-aminocyclopropane-1-carboxylate (intermediate, ACC); and Step III, ACC → Ethylene. These three steps are catalyzed by methionine adenosyltransferase (MAT), 1-aminocyclopropane-1-carboxylate synthase (ACS), and 1-aminocyclopropane-1-carboxylate oxidase (ACO), respectively [9,17,34]. In the present study, tomato ripening was investigated via RNA-Seq analysis to capture accurate information on the process and mechanism at the molecular and genetic levels, which simple genome sequence analysis cannot provide. Tomato fruits in late mature green stage (MG3, right before the breaker stage) were chosen for this study because at this growth stage, the seeds are mature and ready for dispersal. This development drives the fruit to undergo ripening, and thus, the regulation of ethylene production transitions from system 1 to system 2 [10]. The tomatoes in this study were subjected to one of two CO₂ conditions, T1 (5% CO₂, 14 d) or T2 (pure CO₂, 3 h), in order to further understand the role of CO₂ stress on the ripening process.

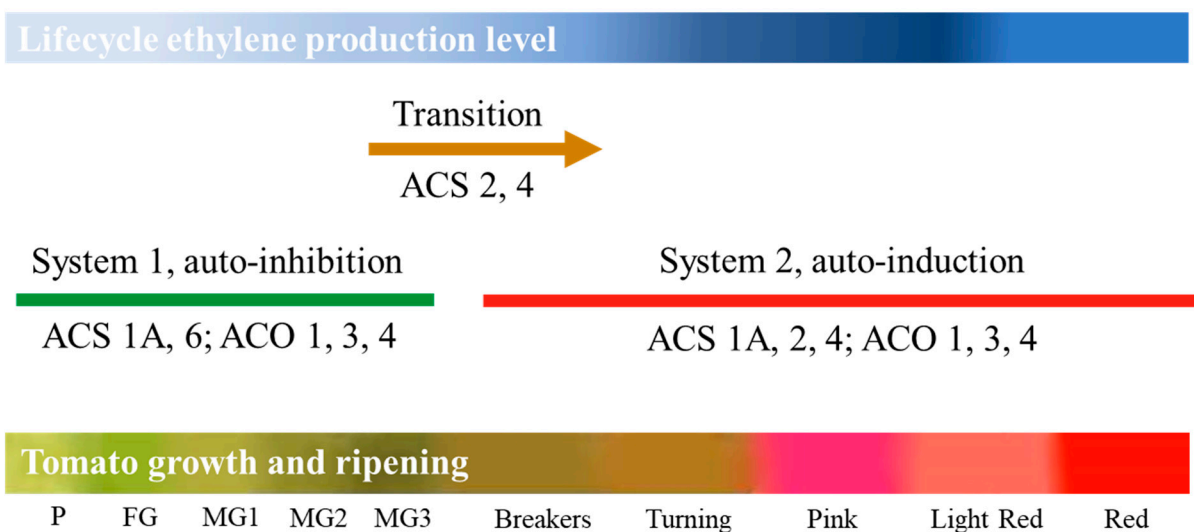


Figure 8. Tomato fruit ripening: regulation of ethylene production and its response.

Although 14 ACS genes and 6 ACO genes have been identified in the tomato genome [17,36–38], only 6 ACS and 6 ACO genes exhibited significantly different expression levels in response to CO₂ treatment in the present study (Figure 5, Table 2). For the T1 group, all genes encoding for ethylene synthesis and signal transduction were significantly downregulated. These results matched well with the ethylene production profile shown in Figure 1a, except for ACO4 synthesis. The higher expression level of the gene Solyc12g099000 revealed that the formation of MAT, step I of ethylene biosynthesis, was the driving force of ethylene production for the tomatoes treated with the T1 method. This was consistent with the finding shown in Figure 4c, where the biosynthesis of amino acids was the most enriched KEGG pathway for tomatoes in the T1 group.

For the T2 group, two important genes encoding for ACS6 and ACS2 were significantly upregulated on d3 and d7, respectively. It is generally accepted that ACS6 is expressed before the onset of tomato ripening and inhibited by ethylene [10,11,39]. In the present experiment, the high expression level of ACS6 at the early stage was accompanied by a large amount of ethylene production (Figure 1a), implying that another mechanism was used to regulate Solyc08g008100 gene expression. Perhaps the 100% CO₂ increased stress so much that there was subsequent overcompensation in ethylene production upon CO₂ removal. On d7, highly expressed ACS2 carried out the transition from S1 to S2; furthermore, ACS2 in combination with ACS4 promoted peak ethylene production. Ethylene regulates ripening by binding to the ethylene receptor and activating signal transduction pathways [10,22]. In comparison with the T1 method, the CO₂ induced by the T2 method further suppressed Solyc09g075440 gene expression and activated the positive regulatory molecule ethylene insensitive 2 (Table 3); all of these factors together impacted ethylene production during the entire process of tomato ripening.

DNA methylation is carried out by DNA methyltransferases; the level of DNA methylation found here varied depending on the ripening stage of the tomatoes. During the development stage of fruit, the promoter regions of the ACS or ACO genes are hypermethylated, while they are demethylated during the ripening stage [10,17]. As reported, transcription starts upstream of the DNA strand adjacent to the promoter sequences; the binding affinity of transcription factors is influenced by chemical modifications of the cytosine or histone groups of DNA [10,17] that result in the modulation of gene transcription. As shown in Table 4, CO₂ induced by T1 treatment activated genes encoding for epigenetic modification on d3 and d7, while the effect of T2 treatment could only be observed on d3. Based on these results, it could be proposed that the introduction of CO₂ using two different treatments resulted in different levels of gene expression due to the methylation and demethylation of DNA promoters, thereby contributing to the inhibition of ethylene production.

The red color of a tomato is indicative of its mature stage, and is due to accumulation of carotenoid metabolites and lycopene in the fruit. The metabolic pathway, which is associated with the degradation of chlorophyll and the transition from xanthophyll to lycopene and carotene, has been studied intensively. A set of genes encoding for the multi-step bioprocess has been verified [26,40–45]. Phytoene formation is the first step of carotenoids biosynthesis. Phytoene is converted into ζ -carotene, and then, to lycopene by desaturase. In the present research, a set of upstream carotenoid enzymes, which catalyze the conversion of geranyl pyrophosphate to phytoene or control the differentiation of organelles, which serve as storage for the carotenoid pigment, were downregulated by T1 treatment on both d3 and d7, but their decrease was only detected on d3 for T2 treatment. Similarly, a difference between T1 and T2 was observed for the downstream genes encoding for carotenoid synthesis enzymes. Carotenoid biosynthesis is subjected to the influence of multiple intrinsic and environmental stimuli. Studies on stimulus-dependent transcriptional regulation have found that light, ethylene, and auxin may play a role in signaling interactions to control tomato carotenoid biosynthesis [46]. Our results show less of a relationship between the ethylene produced and color change, indicating that the regulation mechanism could have been different even though the stimulus was the same, i.e., CO₂, if the stimulus was delivered via different approaches.

Tomato ripening is accompanied by cell-wall degradation and intercellular adhesion weakening, which result in fruit softening. The CO₂ treatment here, either via the T1 or T2 method, delayed tomato ripening, and thus, downregulated enzyme activities that catalyze cell-wall polysaccharide degradation or disrupt cellulose–hemicellulose association, such as galacturonase, pectinase, xylooxidase, expansin, and pectate lyase, among others [19,47]. However, the effect introduced by the T1 method extended to both d3 and d7, while T2 treatment only had an effect on d3, despite the two pectate lyase genes that were upregulated (Figure 1d,e).

The abiotic stress induced by CO₂ treatment affects many aspects of the tomato lifespan, such as mature processing, protein synthesis, DNA synthesis and repair, signal transduction, metabolism and secondary metabolism, and cell differentiation. From the point of view of strength and duration, the effect of stress induced by T1 was recorded on both d3 and d7, while the effect of T2 was observed on d3 in most cases (Figures 1b–e and 4, Tables 4–6). However, ethylene synthesis is the exception (Figure 1a, Tables 2 and 4), where treating the tomatoes with pure CO₂ for only 3 h promoted ethylene production for 12 days via a distinct mechanism that was different from treatment with the T1 method. The treatments with T1 and T2 resulted in distinct gene expression changes, indicating the complexity and inter-dependency of metabolic modification in tomatoes in response to abiotic stress [48–51].

5. Conclusions

The exposure of tomatoes to 5% CO₂ for 14 days (T1) downregulated genes encoding for fruit ripening; the exposure of tomatoes to pure CO₂ for 3 h (T2) upregulated the gene encoding for ACS6, the enzyme responsible for S1 ethylene synthesis, even though there was a large amount of ethylene present, indicating that T1 and T2 regulate tomato ripening via different mechanisms. The two different CO₂ delivery systems resulted in three different patterns of gene expression during tomato ripening. A group of genes was more sensitive to T1, and was either promoted or suppressed. Another group of genes was more sensitive to T2, and was either promoted or suppressed. The third group of genes was not associated with stress intensity and duration; perhaps their activation was the result of a series of genes' cross-actions.

Supplementary Materials: The following supporting information can be downloaded at: <https://www.mdpi.com/article/10.3390/sci5030026/s1>, Figure S1: A volcano plot of significant DGE numbers of CO₂-treated tomatoes on day 7, T1:T2; Figure S2: The most enriched GO terms in T1 vs. T2 on d7. Asterisks (*) indicate $q < 0.05$. Figure S3: KEGG pathway analysis of T2 vs. T1 on d7; brown bars, $q < 0.05$, $p < 0.05$; pink bars, $q < 0.05$, $p > 0.05$. Table S1: Primer sequences used in q-PCR assays. Table S2: Differential Expression of genes due to CO₂ stress (fold change).

Author Contributions: L.L. conceptualized the idea of this research. L.L., J.B., and Y.L. designed the experiments. J.B., Y.L., and L.L. conducted the experiment. L.L., K.K.M., J.B., and Y.L. wrote the manuscript. Y.L., J.A.F., K.K.M., S.S., and S.Z. contributed to conceiving and revising the manuscript. All authors have read and agreed to the published version of the manuscript.

Funding: This work was supported by research project 0500-00093-001-00-D by the United States Department of Agriculture.

Data Availability Statement: Data supporting the results reported in this paper are publicly available on the MDPI webpage upon the paper's acceptance.

Acknowledgments: We are grateful to Amy Ream for helping with the qRT-PCR experiments and to Adrienne Narrowe for producing the heatmap shown in Figure 6.

Conflicts of Interest: The authors declare that the research was conducted in the absence of any commercial or financial relationships that could be construed as potential conflicts of interest.

References

1. Story, E.N.; Kopec, R.E.; Schwartz, S.J.; Harris, G.K. An update on the health effects of tomato lycopene. *Annu. Rev. Food Sci. Technol.* **2010**, *1*, 189–210. [[CrossRef](#)] [[PubMed](#)]
2. Raiola, A.; Rigano, M.M.; Calafiore, R.; Frusciante, L.; Barone, A. Enhancing the health-promoting effects of tomato fruit for biofortified food. *Mediat. Inflamm.* **2014**, *2014*, 139873. [[CrossRef](#)]
3. Kapotis, G.; Passam, H.C.; Akoumianakis, K.; Olympios, C.M. Storage of tomatoes in low oxygen atmospheres inhibits ethylene action and polygalacturonase activity. *Russ. J. Plant. Physiol.* **2004**, *51*, 112–115. [[CrossRef](#)]
4. Kim, J.Y.; Kim, S.-K.; Jung, J.; Jeong, M.-J.; Ryu, C.-M. Exploring the sound-modulated delay in tomato ripening through expression analysis of coding and non-coding RNAs. *Ann. Bot.* **2018**, *122*, 1231–1244. [[CrossRef](#)] [[PubMed](#)]
5. Quinet, M.; Angosto, T.; Yuste-Lisbona, F.J.; Blanchard-Gros, R.; Bigot, S.; Martinez, J.-P.; Lutts, S. Tomato fruit development and metabolism. *Front. Plant. Sci.* **2019**, *10*, 1554. [[CrossRef](#)]

6. Li, T.; Tan, D.; Yang, X.; Wang, A. Exploring the apple genome reveals six ACC synthase genes expressed during fruit ripening. *Sci. Hortic.* **2013**, *157*, 119–123. [CrossRef]
7. Dilshad, S.; Kalair, A.R.; Khan, N. Review of carbon dioxide (CO₂) based heating and cooling technologies: Past, present, and future outlook. *Int. J. Energy Res.* **2020**, *44*, 1408–1463. [CrossRef]
8. Tomasko, D.L.; Li, H.; Liu, D.; Han, X.; Wingert, M.J.; Lee, L.J.; Koelling, K.W. A review of CO₂ applications in the processing of polymers. *Ind. Eng. Chem. Res.* **2003**, *42*, 6431–6456. [CrossRef]
9. Boz, Z.; Welt, B.; Brecht, J.; Pelletier, W.; McLamore, E.; Kiker, G.; Butler, J. Review of challenges and advances in modification of food package headspace gases. *J. Appl. Packag. Res.* **2018**, *10*, 62–97.
10. Singh, P.A.; Wani, A.; Karim, A.A.; Langowski, H.-C. The use of carbon dioxide in the processing and packaging of milk and dairy products: A review. *Int. J. Dairy Technol.* **2012**, *65*, 161–177. [CrossRef]
11. Caleb, O.J.; Mahajan, P.V.; Al-Said, F.A.; Opara, U.L. Modified atmosphere packaging technology of fresh and fresh-cut produce and the microbial consequences—A review. *Food Bioprocess. Technol.* **2013**, *6*, 303–329. [CrossRef] [PubMed]
12. Terai, H.; Tsuchida, H.; Mizuno, M.; Matsui, N. Influence of short-term treatment with high CO₂ and N₂ on ethylene biosynthesis in tomato fruit. *HortScience* **1998**, *33*, 103–104. [CrossRef]
13. Mathooko, F.M. Regulation of ethylene biosynthesis in higher plants by carbon dioxide. *Postharvest Biol. Technol.* **1996**, *7*, 1–26. [CrossRef]
14. De Wild, H.P.J.; Balk, P.A.; Fernandes, A.E.C.A.; Peppelenbos, H.W. The action site of carbon dioxide in relation to inhibition of ethylene production in tomato fruit. *Postharvest Biol. Technol.* **2005**, *36*, 273–280. [CrossRef]
15. May, P.; Liao, W.; Wu, Y.; Shuai, B.; McCombie, W.R.; Zhang, W.Q.; Liu, Q.A. The Effects of Carbon Dioxide and Temperature on MicroRNA Expression in Arabidopsis Development. *Nat. Commun.* **2013**, *4*, 2145. [CrossRef]
16. Thompson, M.; Gamage, D.; Hirotsu, N.; Martin, A.; Seneweera, S. Effects of elevated carbon dioxide on photosynthesis and carbon partitioning: A perspective on root sugar sensing and hormonal crosstalk. *Front. Phys.* **2017**, *8*, 578. [CrossRef] [PubMed]
17. Liu, M.; Pirrello, J.; Chervin, C.; Roustan, J.-P.; Bouzayen, M. Ethylene control of fruit ripening: Revisiting the complex network of transcriptional regulation. *Plant. Physiol.* **2015**, *169*, 2380–2390. [CrossRef]
18. Martín-Pizarro, C.; Posé, D. Genome editing as a tool for fruit ripening manipulation. *Front. Plant. Sci.* **2018**, *9*, 1415. [CrossRef]
19. Gao, J.; Zhang, Y.; Li, Z.; Liu, M. Role of ethylene response factors (ERFs) in fruit ripening. *Food Qual. Saf.* **2020**, *4*, 15–20. [CrossRef]
20. Pereira, L.; Domingo, M.S.; Ruggieri, V.; Argyris, J.; Phillips, M.A.; Zhao, G.; Lian, Q.; Xu, Y.; He, Y.; Huang, S.; et al. Genetic dissection of climacteric fruit ripening in a melon population segregating for ripening behavior. *Hortic. Res.* **2020**, *7*, 187. [CrossRef]
21. Cuesta, G.; Suarez, N.; Bessio, M.I.; Ferreira, F.; Massaldi, H. Quantitative determination of pneumococcal capsular polysaccharide serotype 14 using a modification of phenol–sulfuric acid method. *J. Microbiol. Methods* **2003**, *52*, 69–73. [CrossRef]
22. Bobokalonov, J.T.; Liu, Y.; Shahrin, T.; Liu, L.S. Transcriptomic Analysis on the Regulation of Tomato Ripening by the Ethylene Inhibitor 1-Methylcyclopropene. *J. Plant. Stud.* **2018**, *7*, 49. [CrossRef]
23. Nakatsuka, A.; Murachi, S.; Okunishi, H.; Shiomi, S.; Nakano, R.; Kubo, Y.; Inaba, A. Differential expression and internal feedback regulation of 1-aminocyclopropane-1-carboxylate synthase, 1-aminocyclopropane-1-carboxylate oxidase, and ethylene receptor genes in tomato fruit during development and ripening. *Plant. Physiol.* **1998**, *118*, 1295–1305. [CrossRef] [PubMed]
24. Cantwell, M. Melon Quality and Ripening. In Proceedings of the Fruit Ripening and Retail Handling Workshop Postharvest Technology Center, UC Davis, Davis, CA, USA, 18–19 April 2017; Available online: <https://postharvest.ucdavis.edu/files/261288.pdf> (accessed on 27 May 2023).
25. Gagne, J.M.; Smalle, J.; Gingerich, D.J.; Walker, J.M.; Yoo, S.-D.; Yanagisawa, S.; Vierstra, R.D. Arabidopsis EIN3-binding F-box 1 and 2 form ubiquitin-protein ligases that repress ethylene action and promote growth by directing EIN3 degradation. *Proc. Natl. Acad. Sci. USA* **2004**, *101*, 6803–6808. [CrossRef] [PubMed]
26. Li, J.; Tao, X.; Li, L.; Mao, L.; Luo, Z.; Khan, Z.U.; Ying, T. Comprehensive RNA-seq analysis on the regulation of tomato ripening by exogenous auxin. *PLoS ONE* **2016**, *11*, e0156453. [CrossRef] [PubMed]
27. Cao, D.; Ju, Z.; Gao, C.; Mei, X.; Fu, D.; Zhu, H.; Luo, Y.; Zhu, B. Genome-wide identification of cytosine-5 DNA methyltransferases and demethylases in *Solanum lycopersicum*. *Gene* **2014**, *550*, 230–237. [CrossRef]
28. Zhong, S.; Fei, Z.; Chen, Y.-R.; Zheng, Y.; Huang, M.; Vrebalov, J.; McQuinn, R.; Gapper, N.; Liu, B.; Xiang, J.; et al. Single-base resolution methylomes of tomato fruit development reveal epigenome modifications associated with ripening. *Nat. Biotechnol.* **2013**, *31*, 154–159. [CrossRef]
29. Alelú-Paz, R.; Ashour, N.; González-Corpas, A.; Roperó, S. DNA methylation, histone modifications, and signal transduction pathways: A close relationship in malignant gliomas pathophysiology. *J. Signal. Transduct.* **2012**, *2012*, 956958. [CrossRef]
30. Omidvar, V.; Fellner, M. DNA methylation and transcriptomic changes in response to different lights and stresses in 7B-1 male-sterile tomato. *PLoS ONE* **2015**, *10*, e0121864. [CrossRef]
31. Bolger, A.; Scossa, F.; Bolger, M.E.; Lanz, C.; Maumus, F.; Tohge, T.; Quesneville, H.; Alseekh, S.; Sørensen, I.; Lichtenstein, G.; et al. The genome of the stress-tolerant wild tomato species *Solanum pennellii*. *Nat. Genet.* **2014**, *46*, 1034–1038. [CrossRef]
32. Schwarz, N.; Armbruster, U.; Iven, T.; Brückle, L.; Melzer, M.; Feussner, I.; Jahns, P. Tissue-specific accumulation and regulation of zeaxanthin epoxidase in Arabidopsis reflect the multiple functions of the enzyme in plastids. *Plant. Cell. Physiol.* **2015**, *56*, 346–357. [CrossRef]

33. Kumar, N.; Larkin, J.C. Why do plants need so many cyclin-dependent kinase inhibitors? *Plant. Signal. Behav.* **2017**, *12*, e1282021. [[CrossRef](#)] [[PubMed](#)]
34. Carrari, F.; Baxter, C.; Usadel, B.; Urbanczyk-Wochniak, E.; Zanon, M.-I.; Nunes-Nesi, A.; Nikiforova, V.; Centero, D.; Ratzka, A.; Pauly, M.; et al. Integrated analysis of metabolite and transcript levels reveals the metabolic shifts that underlie tomato fruit development and highlight regulatory aspects of metabolic network behavior. *Plant. Physiol.* **2006**, *142*, 1380–1396. [[CrossRef](#)] [[PubMed](#)]
35. Matas, A.J.; Gapper, N.E.; Chung, M.-Y.; Giovannoni, J.J.; Rose, J. Biology and genetic engineering of fruit maturation for enhanced quality and shelf-life. *Curr. Opin. Biotechnol.* **2009**, *20*, 197–203. [[CrossRef](#)]
36. Li, S.; Chen, K.; Grierson, D. A critical evaluation of the role of ethylene and MADS transcription factors in the network controlling fleshy fruit ripening. *New. Phytol.* **2019**, *221*, 1724–1741. [[CrossRef](#)] [[PubMed](#)]
37. Tiwari, K.; Paliyath, G. Microarray analysis of ripening-regulated gene expression and its modulation by 1-MCP and hexanal. *Plant. Physiol. Biochem.* **2011**, *49*, 329–340. [[CrossRef](#)] [[PubMed](#)]
38. Karlova, R.; Chapman, N.; David, K.; Angenent, G.C.; Seymour, G.B.; Maagd, R.A. Transcriptional control of fleshy fruit development and ripening. *J. Exp. Bot.* **2014**, *65*, 4527–4541. [[CrossRef](#)]
39. Li, T.; Tan, D.; Liu, Z.; Jiang, Z.; Wei, Y.; Zhang, L.; Li, X.; Yuan, H.; Wang, A. Apple MdACS6 regulates ethylene biosynthesis during fruit development involving ethylene-responsive factor. *Plant Cell Physiol.* **2015**, *56*, 1909–1917. [[CrossRef](#)]
40. Liu, L.; Shao, Z.; Zhang, M.; Wang, Q. Regulation of carotenoid metabolism in tomato. *Mol. Plant* **2015**, *8*, 28–39. [[CrossRef](#)]
41. Yuan, H.; Zhang, J.; Nageswaran, D.; Li, L. Carotenoid metabolism and regulation in horticultural crops. *Hort. Res.* **2015**, *2*, 15036. [[CrossRef](#)]
42. Li, X.; Wang, Y.; Chen, S.; Tian, H.; Fu, D.; Zhu, B.; Luo, Y.; Zhu, H. Lycopene is enriched in tomato fruit by CRISPR/Cas9-mediated multiplex genome editing. *Front. Plant. Sci.* **2018**, *9*, 559. [[CrossRef](#)] [[PubMed](#)]
43. Enfissi, E.; Nogueira, M.; Bramley, P.; Fraser, P. The regulation of carotenoid formation in tomato fruit. *Plant. J.* **2017**, *89*, 774–788. [[CrossRef](#)] [[PubMed](#)]
44. Ernesto, B.; Lira, R.B.; Monteiro, S.S.; Demarco, D.; Purgatto, E.; Rothan, C.; Rossi, M.; Freschi, L. Fruit-localized phytochromes regulate plastid biogenesis, starch synthesis, and carotenoid metabolism in tomato. *J. Exp. Bot.* **2018**, *69*, 3573–3586. [[CrossRef](#)]
45. Schouten, R.E.; Farneti, B.; Tijssens, L.M.M.; Alarcón, A.A.; Woltering, E.J. Quantifying lycopene synthesis and chlorophyll breakdown in tomato fruit using remittance VIS spectroscopy. *Postharvest Biol. Technol.* **2014**, *96*, 53–63. [[CrossRef](#)]
46. Cruz, A.B.; Bianchetti, R.E.; Alves, F.R.; Purgatto, E.; Peres, L.E.; Rossi, M.; Freschi, L. Light, ethylene and auxin signaling interaction regulates carotenoid biosynthesis during tomato fruit ripening. *Front. Plant. Sci.* **2018**, *9*, 1370. [[CrossRef](#)]
47. Liu, M.; Diretto, G.; Pirrello, J.; Roustan, J.-P.; Li, Z.; Giuliano, G.; Regad, F.; Bouzayen, M. The chimeric repressor version of an ethylene response factor (ERF) family member, Sl-ERF.B3, shows contrasting effects on tomato fruit ripening. *New. Phytol.* **2014**, *203*, 206–218. [[CrossRef](#)]
48. Marsic, N.K.; Vodnik, D.; Mikulic-Petkovsek, M.; Veberic, R.; Sircelj, H. Photosynthetic traits of plants and the biochemical profile of tomato fruits are influenced by grafting, salinity stress, and growing season. *J. Agric. Food Chem.* **2018**, *66*, 5439–5450. [[CrossRef](#)] [[PubMed](#)]
49. Raffo, A.; Baiamonte, I.; Nardo, N.; Nicoli, S.; Moneta, E.; Peparario, M.; Sinesio, F.; Paoletti, F. Impact of early harvesting and two cold storage technologies on eating quality of red ripe tomatoes. *Eur. Food Res. Technol.* **2018**, *244*, 805–818. [[CrossRef](#)]
50. Wei, Z.; Du, T.; Li, X.; Fang, L.; Liu, F. Interactive effects of elevated CO₂ and N₂ fertilization on yield and quality of tomato grown under reduced irrigation regimes. *Front. Plant. Sci.* **2018**, *9*, 328. [[CrossRef](#)]
51. Zhang, W.-F.; Gong, Z.-H.; Wu, M.-B.; Chan, H.; Yuan, Y.-J.; Tang, N.; Zhang, Q.; Miao, M.-J.; Chang, W.; Li, Z.; et al. Integrative comparative analyses of metabolite and transcript profiles uncovers complex regulatory network in tomato (*Solanum Lycopersicum* L.) fruit undergoing chilling injury. *Sci. Rep.* **2019**, *9*, 4470. [[CrossRef](#)]

Disclaimer/Publisher’s Note: The statements, opinions and data contained in all publications are solely those of the individual author(s) and contributor(s) and not of MDPI and/or the editor(s). MDPI and/or the editor(s) disclaim responsibility for any injury to people or property resulting from any ideas, methods, instructions or products referred to in the content.